5th US Combustion Meeting
Organized by the Western States Section of the Combustion Institute
and Hosted by the University of California at San Diego
March 25-28, 2007.

Prediction of combustion-generated noise in non-premixed turbulent flames using large-eddy simulation

M. Ihme[1]*, H. Pitsch*[1]*, and M. Kaltenbacher*[2]

[1]*Department of Mechanical Engineering,*
Stanford University,
Stanford, CA 94305, USA

[2]*Department of Sensor Technology,*
Friedrich-Alexander-University Erlangen-Nuremberg,
91052 Erlangen, Germany

1 Introduction

Noise generated from technical devices is an increasingly important problem. Jet engines in particular produce sound levels that are not only a nuisance, but may also impair hearing. The noise emitted by such engines is generated by different sources, such as jet exhaust, fans or turbines, and combustion. Increasing restrictions on the allowable noise-emission levels force manufacturers to design quieter engines. This, however, represents a challenging task, because the underlying physical phenomena of the aerodynamic sound generation are yet not entirely understood. Furthermore, design changes made to comply with noise-emission regulations may be accompanied by losses in performance. Numerical simulations offer promise as a tool to address this design challenge, if adequate models are available. Specifically, the large-eddy simulation (LES) technique was demonstrated to be able to predict complex turbulent flow configurations [1–3].

This work addresses the topic of combustion-generated noise at low Mach numbers. A method for the prediction of the acoustic far field pressure emitted by an open non-premixed turbulent flame has been proposed by Ihme *et al.* [4]. This model is based on Lighthill's acoustic analogy [5] and employs a flamelet/progress variable model [6] in modeling the acoustic source-terms. The application of this method is restricted to unconfined flows. In the present work, a hybrid methodology is developed, in which a low Mach number variable-density LES solver is combined with a finite element (FE) code to predict noise generated by combustion. The advantage of this method is that it can be applied to complex flow configurations and that it facilitates an environment for the numerical simulation of practical noise problems.

Kotake [7] and Poinsot & Veynante [8] derived an acoustic analogy from the conservation equations for mass, momentum, and temperature. Because of its strong resemblance to the acoustic

analogy proposed by Phillips [9], we will refer to this analogy as Phillips' equation. Even though the wave operator in this equation does not contain all terms appearing in a moving-media wave equation, this analogy accounts for interactions of the mean flow with the sound [10]. This is different from Lighthill's analogy, since that propagation operator does not account for refraction effects due to the sound speed.

The objective of this paper is the assessment of Phillips' analogy as predictive model for sound generated by turbulent combustion. A key point is the validation of the numerical results with experimental data. The lack of the availability of a comprehensive experimental data set for flow-field quantities and acoustic data for confined geometries limits our application to an open, non-premixed turbulent flame, which has been experimentally studied [11–15]. Special interest is devoted to the analysis of the spatial distribution and temporal behavior of the different source-term contribution in Phillips' analogy.

The remainder of the paper is organized in the following manner. The mathematical model for the hybrid LES/CAA method is presented in Section 2. The experimental configuration, computational setup for the LES, and the acoustic simulation is described in Section 3. Results obtained with the hybrid LES/CAA model are compared in Section 4, followed by conclusions.

2 Acoustic model and FEM formulation

In this section, Phillips' acoustic analogy is presented and major model assumptions are discussed. This equation is solved using an FE formulation. A wave equation accounting for effects of convection and refraction of sound waves by mean flow and inhomogeneities in the media can be derived from the conservation equations of mass, momentum, temperature [7, 8]

$$\mathcal{D}_\tau \rho = -\rho \nabla_{\boldsymbol{y}} \cdot \boldsymbol{u} \,, \tag{1a}$$

$$\rho \mathcal{D}_\tau \boldsymbol{u} = -\nabla_{\boldsymbol{y}} p + \frac{1}{\mathrm{Re}} \nabla_{\boldsymbol{y}} \cdot \underline{\underline{\sigma}} \,, \tag{1b}$$

$$\begin{aligned} \rho c_\mathrm{p} \mathcal{D}_\tau \theta = {} & \frac{1}{\mathrm{Re\,Sc}} \nabla_{\boldsymbol{y}} \cdot (\lambda \nabla_{\boldsymbol{y}} \theta) + \mathrm{Da} \rho \dot{\omega}_\theta + \mathrm{Ec}\, \mathcal{D}_\tau p \\ & + \frac{1}{\mathrm{Re\,Sc}} \left(\rho \alpha \sum_k c_{\mathrm{p},k} \nabla_{\boldsymbol{y}} y_k \right) \cdot \nabla_{\boldsymbol{y}} \theta + \frac{\mathrm{Ec}}{\mathrm{Re}} \underline{\underline{\sigma}} : \nabla_{\boldsymbol{y}} \boldsymbol{u} \,, \end{aligned} \tag{1c}$$

and the ideal gas law

$$p = \frac{1}{\mathrm{Ec}} \rho R \theta = \frac{1}{\gamma} a^2 \rho \,, \tag{2}$$

written in non-dimensional form. Here, $\rho, \boldsymbol{u}, p$, and $\underline{\underline{\sigma}}$, are the density, the velocity vector, the pressure, and the viscous stress tensor, respectively. The dimensionless temperature is denoted by θ, c_p is the specific heat at constant pressure, λ is the heat diffusion coefficient. The substantial derivative is denoted by $\mathcal{D}_\tau = \partial_\tau + \boldsymbol{u} \cdot \nabla_{\boldsymbol{y}}$. The Eckert number is Ec, the Reynolds number is Re, and the Schmidt number is Sc. The gas constant and the variable sound speed are denoted by R and a, respectively. After neglecting terms of order $\mathcal{O}(\mathrm{Ec}, \mathrm{Re}^{-1})$ Eqs. (1b) and (1c) can be written

as

$$\frac{a^2}{\gamma}\nabla_{\boldsymbol{y}}\ln(p) = -\mathcal{D}_\tau \boldsymbol{u}\ , \tag{3a}$$

$$\frac{1}{\gamma}\mathcal{D}_\tau \ln(p) = -\nabla_{\boldsymbol{y}}\cdot\boldsymbol{u} + \mathcal{D}_\tau \ln(R) + \frac{\mathrm{Da}}{c_\mathrm{p}\theta}\dot{\omega}_\theta\ . \tag{3b}$$

Expanding $p = p_\mathrm{ref} + p'$ for small p', and performing the operation $\mathcal{D}_\tau(3b) - \nabla_{\boldsymbol{y}}\cdot(3a)$, leads to the inhomogeneous wave equation. After neglecting convective terms, which is valid for low Mach number flows [8], the simplified equation can be written as

$$\partial_\tau^2 p' - \nabla_{\boldsymbol{y}}\cdot(a^2\nabla_{\boldsymbol{y}}p') = \gamma p_\mathrm{ref}\left[\mathrm{Da}\partial_\tau\left(\frac{\dot{\omega}_\theta}{c_\mathrm{p}\theta}\right) + \partial_\tau^2\ln(R) + \nabla_{\boldsymbol{y}}\boldsymbol{u} : \nabla_{\boldsymbol{y}}\boldsymbol{u}\right]\ . \tag{4}$$

Note that the frequently employed assumption of a constant value for the ratio of specific heats is used. For the methane/air chemistry used here, this assumption is accurate within 10%. The first term on the RHS of Eq. (4) represents an acoustic source-term due to heat release, the second term accounts for effects of temporal variation of the molecular weight of the gas mixture, and the last term is the "shear-refraction term" [10]. It has been pointed out by Goldstein [16] and others that this term, rather than being a source-term, is associated with the propagation of sound waves.

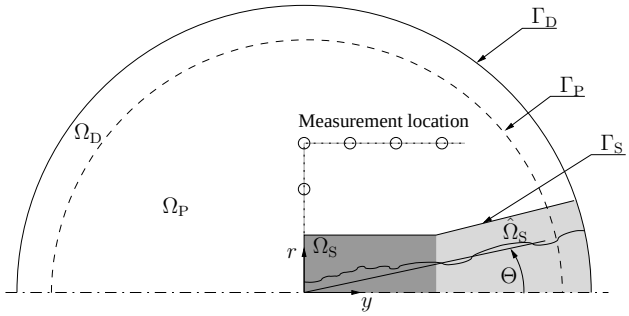

Figure 1: Setup for the acoustic computation: volumes Ω_S, Ω_P, Ω_D and corresponding boundary surfaces Γ_S,Γ_P, and Γ_D. The acoustic source-term is confined to Ω_S and the inhomogeneous source region with the variable sound speed is $\Omega_\mathrm{S}\cup\hat{\Omega}_\mathrm{S}$.

For the FE computation of the acoustic field, the setup schematically shown in Fig. 1 is considered. The domain for the CAA computation is divided into a source region Ω_S, in which the acoustic field is generated; into the region Ω_P, in which the acoustic waves propagate; and into the region Ω_D, where artificial damping and absorbing boundary conditions are applied to approximate the free radiation condition. After transforming Eq. (4) into its weak form

$$\int_\Omega w\partial_\tau^2 p'\mathrm{d}\Omega + \int_\Omega a^2\nabla_{\boldsymbol{y}}w\cdot\nabla_{\boldsymbol{y}}p'\mathrm{d}\Omega - \oint_{\Gamma_\mathrm{D}} a^2 w\nabla_{\boldsymbol{y}}p'\cdot\boldsymbol{n}\mathrm{d}\Gamma = \mathcal{S}+\mathcal{G}+\mathcal{H}\ , \tag{5}$$

with

$$\mathcal{S} = \gamma p_\mathrm{ref}\int_{\Omega_\mathrm{S}} w\nabla_{\boldsymbol{y}}\boldsymbol{u} : \nabla_{\boldsymbol{y}}\boldsymbol{u}\mathrm{d}\Omega\ , \tag{6a}$$

$$\mathcal{G} = \gamma p_\mathrm{ref}\int_{\Omega_\mathrm{S}} w\partial_\tau^2\ln(R)\mathrm{d}\Omega\ , \tag{6b}$$

$$\mathcal{H} = \gamma p_\mathrm{ref}\mathrm{Da}\int_{\Omega_\mathrm{S}} w\partial_\tau\left(\frac{\dot{\omega}_\theta}{c_\mathrm{p}\theta}\right)\mathrm{d}\Omega\ , \tag{6c}$$

this equation is discretized using standard nodal finite elements.

On the outer boundary Γ_{D}, absorbing boundary conditions of first order are applied [17]. Additionally, outgoing pressure waves are smoothly attenuated in a sponge zone using Rayleigh's damping model.

The time discretization is performed by applying an implicit Newmark algorithm, which is unconditionally stable and second order accurate [18].

3 Numerical simulation

3.1 Experimental conditions

The $\mathrm{N_2}$-diluted $\mathrm{CH_4}$-$\mathrm{H_2}$/air flame considered here has been experimentally studied by several authors [11–13]. The burner configuration for the non-premixed flame consists of a central fuel nozzle of diameter D_{ref} which is surrounded by a co-flow nozzle of square shape. The fuel bulk velocity is U_{ref}. Co-flow air is supplied at an axial velocity of $7.11 \times 10^{-3} U_{\mathrm{ref}}$. All reference quantities used in the calculation are given in Table 1 and Ref. [4]. The jet fluid consists of a mixture of 22.1 % methane, 33.2 % hydrogen, and 44.7 % nitrogen by volume with a stoichiometric mixture fraction of $Z_{\mathrm{st}} = 0.167$.

3.2 Numerical setup for LES

The Favre-filtered conservation equations for mass, momentum, mixture fraction, and progress variable are solved in a cylindrical coordinate system using a structured LES code. The geometry has been non-dimensionalized with the jet nozzle diameter D_{ref}. The spatial extend of the computational domain in axial and radial direction is 70×30, respectively. For the discretization of the axial direction, 342 grid points are used, which are concentrated near the nozzle and the grid is coarsened with increasing downstream distance from the nozzle. A section of the fuel pipe with a length of three nozzle diameters is included in the computational domain. For the discretization of this section, 40 evenly spaced grid points are used, corresponding to $\Delta y^+ \approx 45$. The radial direction is discretized by 150 unevenly spaced grid points, with higher resolution in the region of the shear layer. The fuel nozzle is discretized with 27 grid points ($\Delta r^+ \approx 6$ at the wall). The

Table 1: Reference parameters for the reactive jet simulation.

Parameter	Value	Units
D_{ref}	8×10^{-3}	m
U_{ref}	42.2	m/s
ρ_{ref}	1.169	kg/m^2
Re	14,740	-
Sc	0.486	-
Ec	5.4×10^{-5}	-
$\mathrm{M_J}$	0.123	-
Da	0.644	-

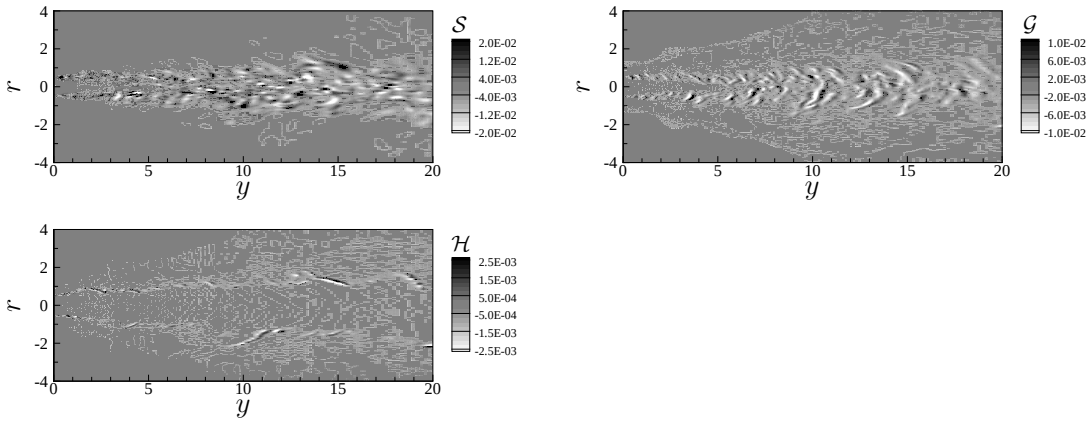

Figure 2: Instantaneous distribution of the shear refraction term ($\mathcal{S}$), the molecular weight term ($\mathcal{G}$), and the chemical source term ($\mathcal{H}$) in Phillips' equation.

non-dimensional minimum and maximum filter widths in the domain are $\Delta_{\min} = 3.32 \times 10^{-2}$ and $\Delta_{\max} = 1.04$.

A turbulent inlet velocity profile is imposed as inflow condition. This profile is obtained by separately performing a periodic pipe-flow simulation. Convective outflow conditions are used at the outlet and slip-free boundary conditions are employed at radial boundaries.

The chemistry is described using the GRI 2.11 mechanism [19], and only stably burning solutions of the steady flamelet equations are used in the flamelet library [4].

3.3 Numerical setup for CAA

For the spatial discretization of the total computational domain, 5.5 million bilinear hexahedral finite elements have been used. According to the minimal wavelength $\lambda_{\min}$, the discretization parameter h is chosen to be $\lambda_{\min}/20$ in Ω_{S} and Ω_{P}, and $\lambda_{\min}/10$ in Ω_{D}. This results in a dispersion error of 0.04% and 0.7%, respectively, under the assumption of non-deformed hexahedral elements [20]. Furthermore, the time step size $\Delta\tau$ has been set to $1/(25\, f_{\max})$, where $f_{\max}$ denotes the highest frequency of the temporally resolved source-term in the LES.

Since the acoustic field simulation and the LES are performed on different grids, the acoustic source-terms are interpolated onto the acoustic grid. This task is done using a bilinear interpolation, and, to keep the interpolation error small, the grid sizes in the source region of the two grids have been generated such that they do not differ very much. In the present case, the ratio of cells on the LES side to cells on the acoustic side was about 1.9 million to one million.

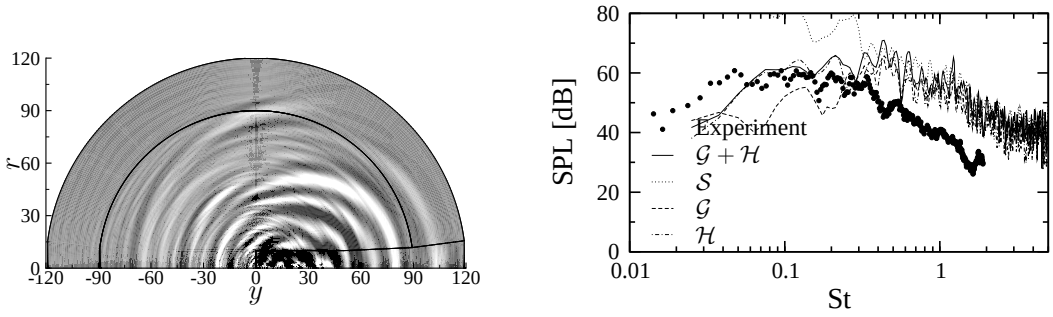

Figure 3: Contour plot of instantaneous pressure fluctuation (left) and comparison of measured and calculated sound pressure level (right).

4 Results

4.1 Source-term analysis

The right hand side in Phillips' equation consists of a heat release term, a source contribution due to local and temporal changes in the molecular weight of the gas mixture, and a shear-refraction term. The instantaneous source-term distribution for Phillips' equation along a constant r-y plane is shown in Fig. 2. The spatial extend of the magnitude of the source-terms decreases for $y > 15$. The contribution of the shear refraction term $\mathcal{S}$ is localized in the turbulent shear layer and the transition region after the potential core closes. The chemical source-term $\mathcal{H}$ is confined to a region that is correlated with the location of stoichiometric conditions.

The spatial distribution of the fluctuating source-term due the variation of the molecular weight of the gas mixture $\mathcal{G}$ indicates the location where the gas composition changes, which is essentially on the rich side of the heat-release region. In the lean region towards the flame, the molecular weight of the mixture is approximately constant, since it is mostly governed by nitrogen. On the rich side, however, the molecular weight changes from that of stoichiometric conditions, which still is mostly determined by nitrogen, to that of the fuel, which can be substantially different. This term is consequently mainly confined to rich flame conditions, and its structure is considerably different from that of the shear-refraction term $\mathcal{S}$.

4.2 Acoustic results

Results obtained using Phillips' equation applied in simulations of the DLR flame are presented and compared with experimental data below.

Figure 3 shows an instantaneous pressure distribution, obtained from the hybrid method using Phillips' equation without shear refraction term. The pressure field has a pronounced radiation in forward direction. The computed sound pressure level (SPL) at a certain measurement location $(x = 0, r = 50)$ is compared with the experiment in the right panel of Fig. 3. Experimental data are denoted by symbols. Phillips' equation with constant sound speed and exclusion of the shear refraction term leads to good agreement in the low frequency range. The sound pressure level for frequencies above St $= 0.3$ is over-predicted. The reason for this discrepancy is under

investigation. Apart from this discrepancy it is shown that the source-term accounting for the variation of the gas constant of the mixture is small compared to the heat release term. Overall, the agreement of the SPL in the low frequency range is in reasonable agreement between experiment and simulation.

5 Conclusions and further work

A hybrid LES/CAA method for the prediction of combustion-generated noise has been developed. The acoustic field is solved using an FE code. The acoustic source-terms obtained from a low Mach number variable-density LES solver are interpolated onto the acoustic grid. For the treatment of the open boundaries in the acoustic domain, absorbing boundary conditions and a sponge layer technique are employed.

The hybrid approach was applied in numerical simulations of an $\mathrm{N_2}$-diluted $\mathrm{CH_4}$-$\mathrm{H_2}$/air flame. The individual acoustic source-terms, appearing in Phillips' equation, were analyzed. Results for the sound pressure level are compared with experimental data. Reasonable agreement between experiments and simulation is obtained for the low frequency range, i.e., for $\mathrm{St} < 0.3$. The sound pressure level at higher frequencies is over-predicted. This discrepancy requires additional investigation.

Further work includes the analysis of the shear-refraction term appearing in Phillips' equation, directivity patterns of the different source-terms, and the quantification of the grid sensitivity of the LES on the acoustic pressure.

Acknowledgments

Funding for this work was provided by the United States Department of Energy within the Advanced Simulation and Computing (ASC) program. Helpful discussions with Profs. Thierry Poinsot, Franck Nicoud, and Sanjiva Lele are gratefully acknowledged.

References

[1] F. di Mare, W.P. Jones, and K.R. Menzies. *Combust. Flame*, 137 (2004) 278–294.

[2] W.W. Kim, S. Menon, and H.C. Mongia. *Combust. Sci. and Tech.*, 143 (1999) 25–62.

[3] P. Moin. *Int. J. Heat Fluid Flow*, 25 (2002) 710–720.

[4] M. Ihme, D. Bodony, and H. Pitsch. *AIAA-2006-2614*, (2006) .

[5] M. J. Lighthill. *Proc. Roy. Soc. London (A)*, 211 (1952) 564–587.

[6] C.D. Pierce and P. Moin. *J. Fluid Mech.*, 504 (2004) 73–97.

[7] S. Kotake. *JSV*, 42 (1975) 399–410.

[8] T. Poinsot and D. Veynante. *Theoretical and Numerical Combustion*. R.T. Edwards, Inc., Philadelphia, PA, 2001.

[9] O. M. Phillips. *J. Fluid Mech.*, 9 (1972) 1–28.

[10] P.E. Doak. *JSV*, 25 (1972) 263–335.

[11] V. Bergmann, W. Meier, D. Wolff, and W. Stricker. *Appl. Phys. B*, 66 (1998) 489–502.

[12] W. Meier, R.S. Barlow, Y.L. Chen, and J.Y. Chen. *Combust. Flame*, 123 (2000) 326–343.

[13] C. Schneider, A. Dreizler, J. Janicka, and E.P. Hassel. *Combust. Flame*, 135 (2003) 185–190.

[14] K. K. Singh, S. H. Frankel, and J. P. Gore. *AIAA Journal*, 41 (2003) 319–321.

[15] K. K. Singh, S. H. Frankel, and J. P. Gore. *AIAA Journal*, 42 (2004) 931–936.

[16] M. E. Goldstein. *Aeroacoustics*. McGraw-Hill, New York, 1976.

[17] A. Engquist, B. & Majda. *Mathematics of Computation*, 31 (1977) 629–651.

[18] T. Hughes. *The Finite Element Method*. Prentice-Hall, New Jersey, 1987.

[19] C.T. Bowman, R.K. Hanson, D.F. Davidson, W.C. Gardiner, V. Lissianski, G.P. Smith, D.M. Golden, M. Frenklach, and M. Goldenberg. GRI-Mech 2.11, 1997. available from `http://www.me.berkeley.edu/gri-mech/`.

[20] M. Ainsworth. *SIAM J. Numer. Anal.*, 42 (2004) 553–575.